Bacterial multispecies invasion of human epithelial bladder cells

Charlotte Abell-King[1,$], Alaska Pokhrel[1], Scott A. Rice[1,2], Iain G. Duggin[1] & Bill Söderström[1,#]

[1] Australian Institute for Microbiology and Infection
University of Technology Sydney
Ultimo NSW, 2007, Australia

[2] Microbiomes for One Systems Health and Agriculture and Food, CSIRO
Westmead NSW, 2145
Sydney, Australia

[$] Current address: Garvan Institute of Medical Research
University of New South Wales
NSW, 2052, Australia

Address correspondence to:
Mail: Bill.soderstrom@uts.edu.au Tel: +61 02 9514 4970

Abstract

Urinary tract infections (UTI) are one of the most common bacterial infections worldwide. While the overall infection course is known on a macroscale, bacterial behavior is not fully understood at the cellular level and bacterial pathophysiology during multispecies infection is not well characterized. Here we establish co-infection models combined with high resolution imaging to compare single- and multi-species bladder cell invasion events in three common uropathogens: uropathogenic *Escherichia coli* (UPEC), *Klebsiella pneumoniae* and *Enterococcus faecalis*. While all three species invaded the bladder cells, under flow conditions the Gram-positive *E. faecalis* was significantly less invasive compared to the Gram-negative UPEC and *K. pneumoniae*. When introduced simultaneously during an infection experiment, all three bacterial species sometimes invaded the same bladder cell, at differing frequencies suggesting complex interactions between bacterial species and bladder cells. Inside host cells, we observed encasement of *E. faecalis* colonies specifically by UPEC. During subsequent dispersal from the host cells, only the Gram-negative bacteria underwent infection-related filamentation (IRF). Taken together, our data suggest that bacterial multispecies invasions of single bladder cells are frequent and support earlier studies showing intraspecies cooperation on a biochemical level during UTI.

Introduction

Urinary tract infections (UTI) are amongst the most common bacterial infections globally [1]. With an estimated 150 million people experiencing an UTI annually [2]. Clinically, UTI are predominantly attributed to only one species of bacteria at a time, with Uropathogenic *Escherichia coli* (UPEC) being the most commonly diagnosed infectious agent at a reported prevalence between 70 and 95% [3-7]. However, it is well established that there are a multitude of different bacterial species present in the bladder environment at any given time [8], and it is known that in acute UTI, polymicrobial infections are common, with both Gram-negative and Gram-positive pathogens present [9,10]. Curiously, multispecies UTI are clinically underdiagnosed, especially if they contain Gram-positive species (*e.g.*, enterococci), and are often disregarded as sample contamination [11]. It was found that in UTIs from 80 female patients with cystitis, that UPEC was over twenty-fold more common than *Enterococcus faecalis* (Gram-positive cocci) as the causative agent of the infections [12]. *E. faecalis* and UPEC are often associated with each other during outgrowth of cultures from UTI [13,14] and *E. faecalis* can suppress the immune activation, promoting UPEC virulence [15]. Recent studies have investigated co-colonization in UTI models [16,17], but very limited information regarding bacterial invasion behaviours under liquid flow conditions simulating the bladder environment is available at high resolution at a single cell level.

Here we use two parallel approaches (‘flow’ and ‘dish’) to investigate differences in human epithelial bladder cell invasion rates of one, two or more bacterial species in the same infection experiment. The first approach is based on a flow channel model with constant exchange of nutrients [18], while the second approach use glass bottom

73 petri dishes under constant orbital agitation. Pathogens used in this study were Gram-
74 negative Uropathogenic *Escherichia coli* (UPEC) and *Klebsiella pneumoniae*, as well
75 as the Gram-positive *Enterococcus faecalis,* as they are the three most commonly
76 found organisms in healthcare-associated UTIs (HAUTIs) [19], and are commonly co-
77 isolated in clinical settings [20], especially in samples from catheter-associated urinary
78 tract infections [21-24]. Challenging the human epithelial bladder cells with various
79 combinations of the bacterial species and examining the system using high-resolution
80 live cell fluorescence microscopy we show, that more than one species of bacteria
81 frequently invades the same bladder cell.
82
83 **Results**
84 *Flow and semi-static agitation affect invasion of human epithelial bladder cells by*
85 *Gram-positive bacteria differently from Gram-negative bacteria.*
86 Initially, we established monospecies infections simulating the invasion phase of
87 uncomplicated UTI using PD07i immortalized human epithelial bladder cells [25,26],
88 challenged with either UPEC (strain UTI89 expressing cytoplasmic mOrange2), *K.*
89 *pneumoniae* (strain TOP52 expressing cytoplasmic mCerulean3) or *E. faecalis* (strain
90 SD234 expressing cytoplasmic GFP), to ascertain whether they were capable of
91 infecting host cells in a previously established *in-vitro* UTI flow-chamber model and to
92 establish baseline infection rates [18,27]. This model is based on a commercial flow-
93 chamber system (IBIDI $I^{0.2}$ μ-Slides connected to NewEra syringe pumps) where
94 constant flow is applied throughout the infection cycle to mimic bladder flow. In parallel,
95 we also used a semi-static infection model using 35 mm glass-bottom Petri dishes
96 under constant orbital agitation (50 rpm). In both models, the bladder cells were initially
97 exposed to a total of ~ 10^7 bacterial cells of each species. All three pathogens invaded

98 the epithelial bladder cells both in the flow-chamber and Petri-dish conditions (Fig. 1a

99 - d).

100

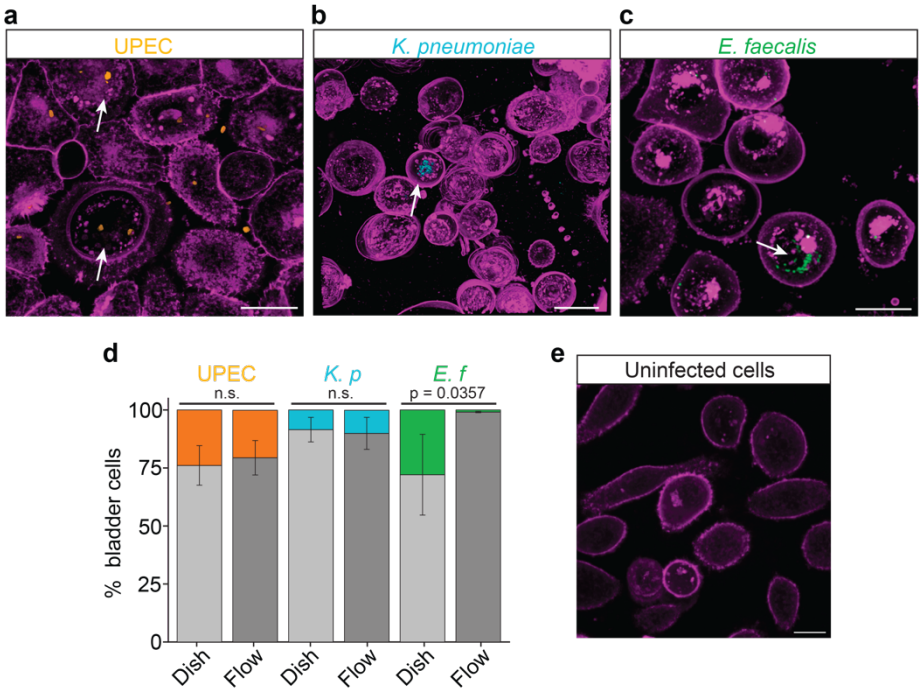

101

102

103 *Fig. 1. Single-species invasion of human epithelial bladder cells using Gram-negative*

104 *and Gram-positive uropathogens.*

105 *Immortalized epithelial bladder cells PD07i (cytoplasmic membranes labelled with*

106 *CellBright650, magenta) grown on a 35-mm glass bottom petri-dish or in a flow*

107 *chamber were infected by either* ***a****, UPEC (strain UTI89 expressing cytoplasmic*

108 *mOrange2);* ***b****,* K. pneumoniae *(strain TOP52 expressing cytoplasmic mCerulean3);*

109 *or* ***c****,* E. faecalis *(strain SD234 expressing cytoplasmic GFP). White arrows indicate*

110 *internalised bacteria.* ***d****, Proportion of bladder cells infected (colour) and uninfected*

111 *(grey) in various conditions and bacterial species. Graphs are based on values from 3*

112 *infections for each condition. n.s. = not statistically significant. $p < 0.05$ = statistically*

113 *significant. K. p* = K. pneumoniae*. E. f* = E. faecalis*. Dish = 35 mm glass bottom petri-*

114 *dish. Flow = 15 μl min^{-1} in flow channel (IBIDI μ-Slide I$^{0.2}$).* ***e****, PD07i cells maintained*
115 *without bacteria. Images are from petri-dish experiments. Scale bars = 20 μm. Note*
116 *that the bottom layers containing only epithelial membrane of the Z-stacks were*
117 *omitted for better visualization of internal bacteria.*
118
119 At 20 h post inoculation, UPEC had invaded the most bladder cells of the tested Gram-
120 negative species (23.9 ± 8.5 % of the bladder cells in the semi-static petri dish model
121 and 20.6 ± 7.4% in the flow model, Mean ± S.D., n > 432 from three independent
122 infection experiments), while *K. pneumoniae* invaded approximately half of this
123 number (8.49 ± 5.3% in the dish model and 10 ± 6.9 % in the flow model, n > 321 from
124 three independent infections of each condition) (Fig. 1d). *E. faecalis* showed the
125 highest overall invasion with an average 27.9 ± 17.4% of the bladder cells invaded in
126 the dish model (n = 335, from 3 experiments) (Fig. 1d). In contrast, *E. faecalis* invaded
127 less than 1% of the bladder cells under the flow-chamber conditions (n = 462, from 3
128 independent experiments). For UPEC and *K. pneumoniae* the variations between the
129 models were statistically nonsignificant, while for *E. faecalis* they were p = 0.0357
130 (statistically significant).
131
132 *Elevated invasion rates for UPEC in dual species infection with* E. faecalis*.*
133 Since so few bladder cells were invaded by *E. faecalis* in the flow-chamber model, the
134 culture-dish model was mainly used to follow invasion during multispecies UTI. We
135 co-inoculated the bladder cells with equal numbers of UPEC and *E. faecalis* (a
136 combined total of ~ 10^7 bacteria [15]). Based on images of more than 560 randomly
137 inspected bladder cells at ~ 20h post inoculation (regions of interest [ROIs] were
138 chosen based on fluorescence signal from bladder cell membranes, and Z-stacks

139 were acquired for each ROI) from three independent experiments, almost half (~ 45%,

140 Fig. 2a - b) were invaded by at least one type of bacterial species. Most infected

141 bladder cells were only invaded by one species (Fig. 2a, arrows).

142

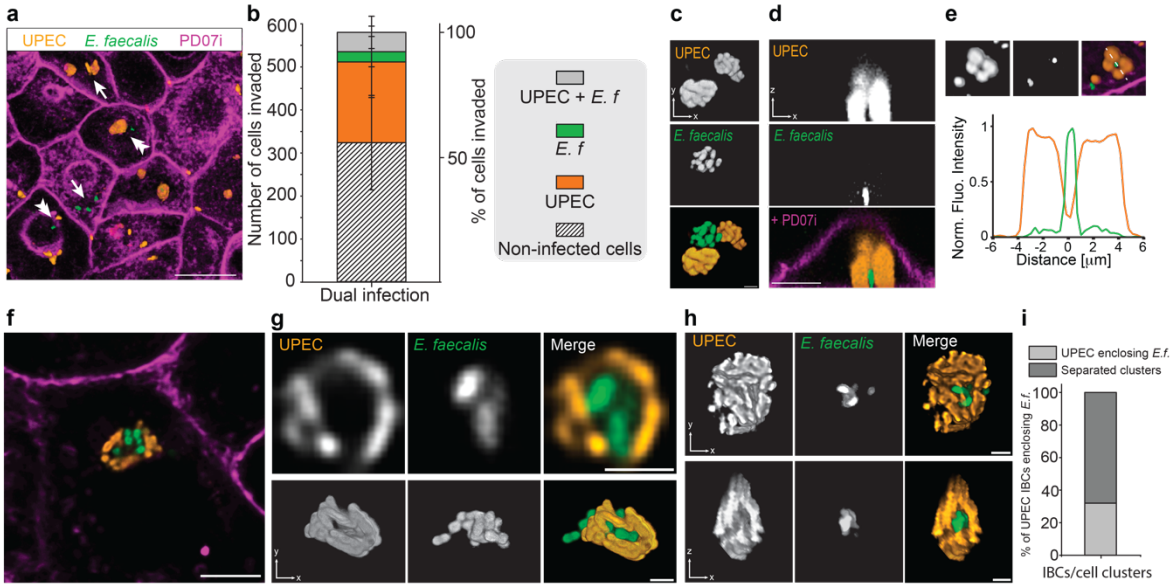

143

144 *Fig. 2. Bladder cell invasion during* UPEC *and* E. faecalis *co-infections.*

145 ***a**, PD07i (membranes labelled with CellBright 405 or 650) cells co-infected with* UPEC

146 *(orange) and* E. faecalis *(green). Scale bar 20 = µm.* ***b**, ratio of invaded PD07i cells.*

147 *E. f = E. faecalis* ***c**, Typical intracellular* UPEC *(orange) and* E. faecalis *(green) clusters.*

148 UPEC *appeared more tightly packed than* E. faecalis*. Scale bar 1 µm.* ***d** and **e**, Low*

149 *resolution Z-stacks showing UPEC surrounding* E. faecalis *in co-invaded PD07i cells.*

150 *Scale bar **d** = 5 µm. The graph in **e** shows fluorescence intensity traces for the white*

151 *dash line in the image above. UPEC (orange) and* E. faecalis *(green). Dotted scale*

152 *line = 12 µm.* ***f**, **g** and **h**, Representative single images and confocal 3D*

153 *reconstructions of* E. faecalis *(green) surrounded by UPEC (orange). Scale bar **f** = 10*

154 *µm. Scale bars **g**, **h** = 2 µm.* ***i**, Percentage of dual invaded PD07i cells with UPEC cells*

155 *enclosing* E. faecalis cells *(as shown in **g** and **h**). Note various orientations of*
156 *reconstructed Z-stacks.*
157
158 In these dual-species infections, UPEC alone were internalised in 33% of cells
159 (compared to ~ 24 % in single species dish infections [Fig. 1d]), whereas *E. faecalis*
160 alone were internalised in only 4% (Fig. 2b) (compared to ~ 28% in single species dish
161 infections [Fig. 1d]). The percentage of bladder cell invasions of either or both bacteria
162 in dual-species infections was almost 45% (43.6 ± 19.3% (n = 564 cells, from 3
163 experiments)). Surprisingly to us, a relatively high number, 44 of 564 or approximately
164 8% of the individual bladder cells were invaded by both bacterial species at the same
165 time (Fig. 2a, arrow heads).
166 We noticed that the arrangement of the internalised bacteria was distinct for each
167 species; UPEC formed condensed IBCs as previously established [28], while *E. faecalis*
168 were often organized in more loosely organised clusters in which single cells were
169 readily resolved (Fig. 2c). Initial 3D reconstructions of low-resolution images
170 suggested that UPEC clusters were often in close spatial proximity of the *E. faecalis*
171 cells (Fig. 2d - e). With increased resolution, it became evident that tightly packed
172 UPEC cells formed multicellular communities that frequently surrounded one or a few
173 *E. faecalis* cells (Fig. 2f - h). This type of UPEC 'encirculation' of *E. faecalis* cells was
174 apparent in a substantial fraction of the total observed UPEC IBCs (32%) during dual
175 species invasion (Fig. 2i). We speculate that *E. faecalis* and *E. coli* might cooperate to
176 increase the likelihood of prolonged infection [15].
177
178 *Lower overall infection rates of bacteria in dual and triple-species infections when* K.
179 pneumoniae *is present.*

To investigate whether other mixed bacterial cultures would co-invade PD07i cells and exhibit similar interactions as seen for UPEC / *E. faecalis*, we carried out infection experiments with other combinations of bacteria: *E. faecalis* and *K. pneumoniae* (Gram-positive/Gram-negative pair), UPEC and *K. pneumoniae* (Gram-negative/Gram-negative pair) or all three species (UPEC, *E. faecalis* and *K. pneumoniae*). At 20h post inoculation, we detected host cells containing all combinations of the bacteria investigated (Fig. 3a – c), but the invasion frequencies varied substantially.

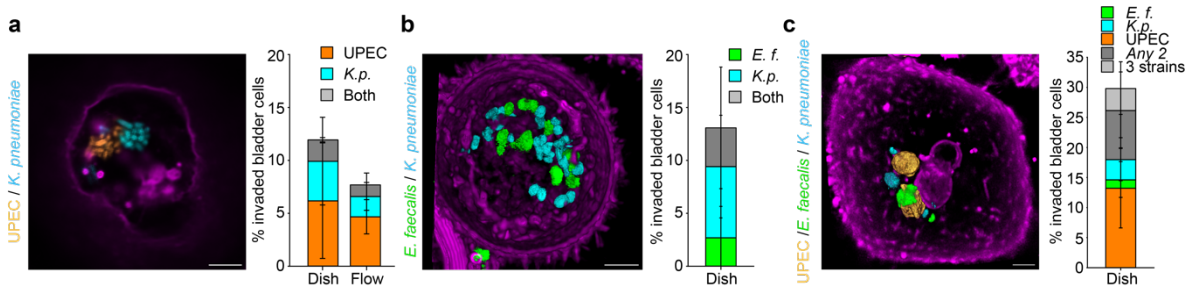

Fig. 3. Prevalence of bacterial invasion in dual- and triple-species infections. Representative images of PD07i cells invaded by ***a****,* UPEC *and* K. pneumoniae *(2D confocal image); % of invasion (n = 519), Dish:* UPEC *6.1 ± 5.4 % (mean ± S.D.) , K.p. 3.7 ± 4.2 %, both 2 ± 2.2 %. Flow:* UPEC *4.6 ± 2.6 %, K.p. 1.9 ± 1.8 %, both 1.35 ± 1.9 %.* ***b****,* E. faecalis *and* K. pneumoniae *(deconvolved 3D-reconstruction of a confocal Z-stack, n = 463). % of invasion: E.f 2.7 ± 3 % , K.p. 6.8 ± 4.9 %, both 3.7 ± 5.8 %.* ***c****,* UPEC, E. faecalis *and* K. pneumoniae *(deconvolved 3D-reconstruction of a confocal Z-stack, n = 349). % of invasion: UPEC 13.3 ± 6.7 %, E.f 1.3 ± 3 %, K.p. 3.4 ± 3.6 %, Any 2 species 8.2 ± 6.4 %, all 3 strains 3.7 ± 4.4 %. PD07i membranes labelled with CellBright 650. Scale bars = 4 μm. E. f* = E. faecalis. *K. p* = K. pneumoniae. *Note, different scales on y-axis.*

201

202 In contrast to the UPEC / *E. faecalis* case, encirculation was not observed when
203 *E. faecalis* was co-infected with *K. pneumoniae* (4 independent infection experiments,
204 n = 463 cells in total), nor when the two Gram-negative species UPEC and *K.*
205 *pneumoniae* were used in the same infection (4 independent infection experiments, n
206 = 519 cells in total). UPEC and *K. pneumoniae* often formed dense IBCs adjacent to
207 one another but did not encase or mix with each other (Fig. 3a). Overall, UPEC and
208 *K. pneumoniae* invaded ~ 12% of all bladder cells in the Dish model and ~ 8% of all
209 bladder cells in the flow channel model, however they coinfected only 1 - 2% of bladder
210 cells both in either model (Fig. 3a).
211 During *E. faecalis* and *K. pneumoniae* co-infection, we noticed that while they were
212 capable to co-invade bladder cells, we did not observe dense IBCs (Fig. 3b). *E.*
213 *faecalis* has previously been shown to antagonize *K. pneumoniae* biofilm formation
214 during mixed growth albeit under different conditions compared to the intracellular
215 conditions in the present study [29]. The total percentage of invaded bladder cells in a
216 *E. faecalis* and *K. pneumoniae* dual species combination was ~ 13%, with 3.7% of all
217 observed of bladder cells invaded by both (Fig. 3b).
218 For three-species infections (UPEC, *E. faecalis* and *K. pneumoniae)*, UPEC / *E.*
219 *faecalis* again showed similar organizational patterns as they did in two species
220 infections, while *K. pneumoniae* was predominately localized separate from the other
221 two (Fig. 3c). In the three species infections roughly 30% of bladder cells were invaded
222 by at least one species, with almost 4% invaded by all three (Fig. 3c, n = 349, 3
223 independent infection experiments). This was less than the invasion frequency of the
224 UPEC / *E. faecalis* dual infections where ~ 45% of the bladder cells were invaded by

225 at least one type of bacteria (Fig. 2b), suggesting that *K. pneumoniae* could have an
226 antagonistic effect on invasion efficiency during multi-species infections.
227
228 *Gram-negative bacteria undergo infection-related filamentation in multispecies*
229 *infections, while Gram-positive do not.*
230 During murine model UTI, UPEC have been seen to undergo morphological changes
231 during intracellular bacterial community (IBC) formation and dispersal, where UPEC
232 grow into long filamentous cells [30]. These morphologies were later also seen in female
233 patents with cystitis [12] and more recently also confirmed in flow-chamber models using
234 human bladder cells and urine [18,27,31,32]. To determine whether single and multi-
235 species co-infections undergo the same morphological changes under the established
236 conditions, we next visualized cells sampled after the dispersal stage of infection by
237 exposing infections to human urine (20 h) [18,27]. Both UPEC and *K. pneumoniae* formed
238 filaments of several hundreds of microns long (Fig. 4a - b). For *K. pneumoniae*, similar
239 morphology cycles have been previously observed in murine models [33], but not in *in-*
240 *vitro* models using human epithelial bladder cells and urine. The average length of
241 both UPEC and *K. pneumoniae* filaments from infections was ~ 50 μm (Fig. 4d). By
242 comparison, UPEC and *K. pneumoniae* rods grown in LB medium were approximately
243 3.5 μm (Fig. 4d). We classified cells as filaments if they were at least two times the
244 average WT cell length, *i.e.*, 7 μm. We observed that the number of cells that
245 underwent filamentation (but not the average length of filaments) was lower in the dish
246 model compared to the flow-chamber model. While the molecular reasons for this is
247 not currently clear, we speculate that proficiency of morphology changes may be
248 connected to flow and shear-force dynamics, or the continual exchange of constituents
249 in the medium [31]. In contrast to the Gram-negative species, *E. faecalis* cells did not

250 filament or grow significantly larger upon exposure to human urine (Fig. 4c, 4d).
251 Average lengths after an infection were ~ 1.4 μm (n = 215) from petri-dish infection
252 and ~ 1.6 μm (n = 102) from flow chambers which was similar to lengths for *E. faecalis*
253 cells grown in BHI medium only (1.75 (n = 238)) (Fig. 4d). Similar results for
254 filamentation were observed during triple-species infections (Fig. 4e). Taken together,
255 these observations suggest that infection-related filamentation may be a broadly
256 occurring phenomenon in uropathogenic Gram-negative bacteria and it also transpires
257 during multispecies infections.
258

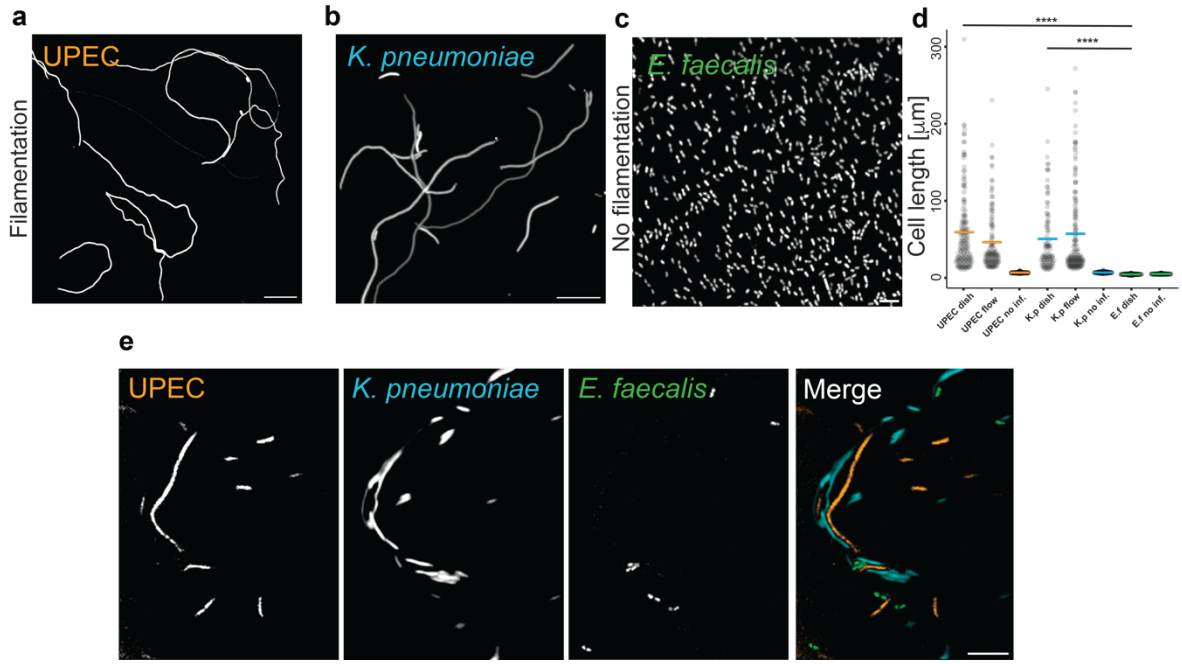

259
260

261 *Fig. 4. Gram-negative, but not Gram-positive, species undergo infection-related*
262 *filamentation in both single and multi-species infections.*
263 *Representative images of bacteria after being exfoliated from PD07i cells during single*
264 *species infections.* ***a****,* UPEC*,* ***b****,* K. pneumoniae*,* ***c****,* E. faecalis*. Note all strains retain*
265 *their fluorescence throughout invasion and exfoliation.* ***d****, Average lengths of bacterial*
266 *filaments* (UPEC and K. pneumoniae*) and cells* (E. faecalis*) after 20 h of urine*

267 *exposure during infections. The average length of* UPEC *filaments was 56.0 ± 59.9*
268 *μm (n = 158) in dishes, and 43.3 ± 40.05 μm (n = 122) in flow.* K. pneumoniae
269 *filaments were 47.3 ± 45.3 μm (n = 98) in dishes and 54 ± 57.8 μm (n = 156) in flow*
270 *and.* UPEC *and* K. pneumoniae *rods grown in LB media were on average 3.46 ± 0.69*
271 *μm (n = 187) and 3.62 ± 0.76 μm (n = 192), respectively. Average lengths of* E. faecalis
272 *after an infection were 1.42 ± 0.4 μm (n = 215) from petri-dish infection and 1.59 ±*
273 *0.41 μm (n = 102) from flow chambers. Lengths for* E. faecalis *cells grown in BHI*
274 *media only was 1.74 ± 0.31 μm (n = 238). Dish = 35-mm glass bottom petri-dish.*
275 *Flow = 15 μl min^{-1} in flow chamber (IBIDI I$^{0.2}$).* ***e****, Filamentation of* UPEC *and* K.
276 pneumoniae *but not* E. faecalis *during a representative three species infections. Scale*
277 *bars A, B and E = 10 μm, C = 4 μm.*
278
279 Discussion
280 Numerous studies have investigated UTI microbial interactions and biofilm formation
281 *in-vitro* in liquid media (*e.g.*, rich media, synthetic or human urine) and on catheters
282 [34-37], their effect on immune activation[15,17,38,39] , and *in-vivo* in animal models[40-42] (a list
283 on further reading here: [8]). However, hardly any studies have looked at bacterial co-
284 invasion behaviour at single bladder cell level. Here, to study and better understand
285 bacterial invasion during multispecies UTI on single cell levels in a systematic way, we
286 established a set of multi-species UTI *in-vitro* models. We visually compared invasion
287 frequencies of three common urinary tract pathogens, Uropathogenic *Escherichia coli*
288 (UPEC), *K. pneumoniae* and *E. faecalis,* using human bladder cell *in-vitro* infection
289 models under two different conditions ('flow' and 'dish'). In the flow condition, UPEC
290 showed highest overall invasion frequency, followed by *K. pneumoniae*, while *E.*
291 *faecalis* hardly invaded any bladder cells. Differences in invasion frequency between

292 UPEC and *K. pneumoniae* has been observed previously in murine models, and was
293 attributed differences in adhesion capabilities through lower type 1 pilus expression of
294 *K. pneumoniae* [33]. The invasion frequencies of UPEC and *K. pneumoniae* were only
295 marginally impacted by switching from continuous flow to circular agitation. On the
296 other hand, the Gram-positive *E. faecalis* exhibited a large variation in invasion
297 frequency between the models tested in this study. While *E. faecalis* is a well-
298 established uropathogen [43,44], our observations suggest a weakened ability to adhere
299 and invade bladder cells under the flow conditions in our model. At this point we do
300 not fully understand the details resulting in the large variation in bladder cell invasion
301 of *E. faecalis* between our flow and dish models, but similar behaviours have
302 previously been linked to the reduced adherence capabilities of *E. faecalis* [11,43,45,46].
303
304 In multispecies infection experiments, we show that multiple species of bacteria can
305 invade the same bladder cell. While molecular details governing intracellular
306 coexistence of bacteria during UTIs remains elusive, our observations indicate that
307 whenever UPEC and *E. faecalis* are introduced together the overall rate of infection
308 increases. Similar cooperation and increase in pathogenicity by UPEC and *E. faecalis*
309 have been suggested based on results from murine models [15]. The observation that
310 UPEC readily encirculate *E. faecalis* is perplexing and its biological significance is
311 unclear but suggests a spatial importance of the previous observations that these two
312 species cooperate on a biochemical level to increase pathogenesis [40,42,47,48].
313 In contrast, whenever *K. pneumoniae* was introduced into a multispecies infection
314 situation was the average invasion frequency always lower than in the corresponding
315 single species infections. Supporting this observation, *E. faecalis* has previously been
316 implicated in suppressing *K. pneumoniae* growth during polymicrobial biofilm

formation in human urine [29]. This suppression by *E. faecalis* seems also be extended to other Gram-negative species (*i.e.*, *Pseudomonas aeruginosa*) [49].

Both infection models presented in this study caries its own merits, and each may be favoured depending on the research question in mind, *e.g.,* 'Flow' could represent bladder release, while 'Dish' would possibly depict a resting bladder situation. We believe that the observations presented in this study will initiate a spark for further investigation into detailed genetics studies exploring dedicated signalling pathways and potential quorum sensing in multispecies UTIs at a single cell level. This will undoubtably play an increasingly important role in understanding competing or cooperative behaviours of bacteria during infections as antimicrobial resistance continue to rise.

330 **Materials and Methods**

331

332 **Human Ethics**

333 This study was approved by the UTS Human Research ethics committee with approval
334 numbers HRCH REF No. 2014000452 and HREC ETH22-7590. All urine doners gave
335 their approval to participate in this study by informed consent under this study's ethics
336 approval numbers above.

337

338 **Plasmid construction**

339 pCAK1 and pAP1 plasmids were constructed by replacing the GFP sequence in pGI5
340 [18] with mCerulean3 and mOrange2 sequences, respectively. The mCerulean3 and
341 mOrange2 gene fragments were amplified from pEB1-mCerulean3 and mOrange2-
342 pBAD plasmids, both obtained from Addgene (Addgene plasmids #103973 and
343 #54531) [50,51]. To construct pCAK1 and pAP1, pGI5 was digested with *Nco*I and *Bam*HI,
344 and assembled with mCerulean3 and mOrange2 PCR products containing 20-30 bp
345 homologous regions from pGI5 on both the ends. This was performed using a *in vivo*
346 DNA assembly method [52]. The final products were confirmed by Sanger sequencing
347 and fluorescence microscopy.

348

349 **List of Primers**

mCerulean3_FW	GCC CGG TCT AGA GGA GGT ACT ACC ATG AGT AAA GGA GAA GAA CTT TTC ACT
mCerulean3_RV	GGT CGA CGG ATC TTT AGG ATC CTT TTA TTT GTA TAG TTC ATC CAT GCC ATG

mOrange2_FW	CGG TCT AGA GGA GGT ACT ACC ATG GTG AGC AAG GGC GAG GAG
mOrange2_RV	CAG GTC GAC GGA TCT TTA GGA TCC TTA CTT GTA CAG CTC GTC CAT GCC

350

351 **Bacterial growth**

352 Bacterial strains were used as follows: Uropathogenic *Escherichia coli* UTI89
353 transformed with mOrange2 (pAP1) or mCherry (pGI6) [53], *Klebsiella pneumoniae*
354 TOP52 transformed with mCerulean3 (pCAK1) or sfGFP (pGI5), and *Enterococcus*
355 *faecalis* OG1RF expressing GFP from the chromosome [54]. All fluorescent proteins
356 were produced as constitutively expressed freely diffusing molecules in the
357 cytoplasms of the corresponding bacterial strain. A single colony of respective strain
358 was grown overnight in a 20 ml Luria Broth (*E. coli* and *K. pneumoniae*) or Brain Heart
359 Infusion (*E. faecalis*) culture at 37°C without shaking to induce expression of type-1
360 pili which facilitates adhesion to the bladder cells during infection. Antibiotics were
361 added when appropriate (Spectinomycin 50 µg ml^{-1}, Rifampicin 100 µg ml^{-1}). The
362 following morning, the cultures were pelleted and resuspended in 1 x PBS added to
363 the infection model.

364

365

366

367

368

369

370

371 *Table 1: Bacterial species used in this study.*

Species	Strain	Source	Fluorescent Protein	Plasmid Or Chromosome
E. faecalis	OG1RF	Prof. Garsin (Uni Texas)	GFP	Chromosome
UPEC	UTI98	Lab strain	mOrange2	Plasmid (pAP1) -this study
UPEC	UTI98	Lab strain	mCherry	Plasmid(pGI6) [53]
K. pneumoniae	TOP52	Prof. Hultgren (Uni Washington)	mCerulean3	Plasmid (pCAK1) -this study
K. pneumoniae	TOP52	Prof. Hultgren (Uni Washington)	sfGFP	Plasmid(pGI5) [18]

372

373 **Bladder cell growth**

374 Immortalized Epithelial bladder cells (PD07i [25,26]) were grown and maintained in
375 EPILIFE media supplemented with Human Keratinocyte Growth supplement (HKGS)
376 in 5% CO_2 at 37 °C. Cells were split as required using standard Trypsinization methods
377 upon reaching ~ 80% confluency.

378

379

380

381 **Human urine preparation**

382 Human urine was collected from both male and female donors. Samples were
383 collected in the mornings and stored at 4 °C for at least 2 days before further
384 processing. Samples were pelleted at 3000 rpm, the supernatant filtered through a 0.2
385 μm filter and aliquoted into 50 ml falcon tubes before placed in – 20 °C for storage
386 until use. Urine was only used if the pH was between 5 - 6.5 and the Urine Specific
387 Gravity (USG) was in the range between 1.024 to 1.030, values that has been shown
388 to produce high degree of filamentation [18,27].

389

390 **Infection models**

391 *Flow model*

392 The *in-vitro* UTI flow channel model has been described previously [18,31]. Here only
393 slight changes were introduced as follows, μ-Silde $I^{0.2}$ Luer (IBIDI #80166, total
394 channel volume 50 μl) flow channels were seeded with bladder cells according to the
395 manufacturer's recommendations. The channels were connected to a New Era pump
396 system for continuous flow of nutrients, this was left to run until a confluent layer of
397 bladder cells formed [27]. Bacterial cells resuspended in PBS at an OD_{600} of 0.2 - 0.4
398 were introduced fully in the flow channels and flushed at a flow rate of 15 μl min^{-1} for
399 10-15 minutes (resulting in a total of ~10^7 bacterial cells run over the bladder cells
400 depending on concentration and species, as determined by CFU counts), before fresh
401 EPILIFE media again was flown over the cells for 7 hours (initial 10 minutes at 100 μl
402 min^{-1} to flush out excess bacteria, then 15 μl min^{-1} for the reminder of the time) to allow
403 for invasion. After this, the media was exchanged to EPILIFE containing Gentamycin
404 (f.c. 100 μg ml^{-1}[18], for the dual infection of UPEC and *K. pneumoniae* was on additional
405 100 μg ml^{-1} of Ampicillin added) for 13 hours to eliminate all extracellular bacteria. To

406 monitor formation of intracellular bacterial communities, channels were taken to the
407 microscope for imaging at this point. Immediately prior to imaging, bladder cell
408 membranes were stained with CellBrite405 or 650 in PBS (f.c. 1:100, with the addition
409 of CellBrite Enhancer to mask intracellular fluorescence according to the
410 manufacturer's recommendations) under flow (15 μl min^{-1}) for 40 minutes, and washed
411 twice with 1 x PBS. Channels were re-filled with EPILIFE media to sustain cell health
412 during imaging.
413 To generate filaments, after subjecting samples to the EPILIFE/antibiotics mixture,
414 human urine was added to the flow system (15 μl min^{-1}) for 20 hours. Bacterial
415 samples were collected through the back-end of the flow channels, washed once in 1
416 x PBS, resuspended in LB or BHI. 4 μl of respective culture was placed on 2 % agarose
417 pads (w/w) and directly taken for imaging.
418
419 *Dish model*
420 In the semi-static infection model a similar experimental workflow was followed as for
421 the flow model with the same time intervals in changing media, with the exception that
422 all steps were carried out in a 35 mm Petri dish (IBIDI glass bottom dish with glass
423 coverslip bottom (#1.5), pre-sterilized, cat number #81218-200) placed in a CO_2
424 incubator at 37 °C with 50 rpm orbital agitation. For the dish models the total amount
425 of bacteria (~10^7 , roughly corresponding to an MOI of 100) was distributed evenly
426 over the bladder cells at one time point only. Bacteria were incubated for 15 minutes
427 before liquid was aspirated of and fresh EPILIFE media (2 ml) was added and grown
428 for 7 hours. Following this, media was exchanged to EPILIFE containing Gentamycin
429 (f.c. 100 μg ml^{-1}[118]), for 13 hours to eliminate all extracellular bacteria. To monitor
430 formation of intracellular bacterial communities, channels were taken to the

431 microscope for imaging. Immediately prior to imaging were bladder cell membranes
432 stained with CellBrite405 or 650 in PBS (f.c. 1:100, with the addition of CellBrite
433 Enhancer to mask intracellular fluorescence according to the manufacturer's
434 recommendations) for 40 minutes, washed twice in 1 x PBS and again covered with 2
435 ml EPILIFE to sustain cell health during imaging.
436 To generate filaments in the Petri dish model, 1 ml urine was added and manually
437 exchanged once an hour for the first 4-5 hours before a final resuspension of 3 ml was
438 done and left in the incubator for 15 hours.
439
440 **Imaging**
441 To minimise biased imaging, regions of interest [ROIs] were chosen based on
442 fluorescence signal from bladder cell membranes only, and Z-stacks were acquired
443 for each ROI. Imaging was performed on a Leica Stellaris confocal microscope
444 equipped with a 63x oil objective enclosed in an environmental chamber operated at
445 37 °C and 5 % CO_2 (Oko-Lab). The fluorophores were excited by a white laser at
446 optimized wavelengths, and emission was collected in pre-set system optimised
447 detector intervals for AlexFluor405, mCerulean3, EGFP, mOrange2 and
448 AlexaFluor647 depending on experiment, to minimize channel crosstalk. Z-stacks
449 were always acquired to validate that the bacteria in fact were inside the bladder cells.
450 Image size was either 2048 x 2048 or 4096 x 4096, with pixel size 90 and 45 nm,
451 respectively. The pinhole was set to 1 AU and Z-stacks were collected with software
452 optimized step length of either 125 or 250 nm (30-99 images per stack, depending on
453 step length and thickness of the bladder cell in question). 3D reconstruction and
454 deconvolution of Z-stacks were performed in the Leica LAS software and further
455 visualised in FIJI (ImageJ).

456

457 **Quantification and statistical analysis**

458 Raw microscopy images, deconvoluted Z-stacks and movies were transferred to FIJI
459 (ImageJ) for final analysis and processing. Fluorescence traces were analysed in
460 OriginPro 2021 (V. 9.8.0.200 [Academic]). Note that all fluorescence traces were
461 generated from raw microscopy data and not deconvoluted data. Cell lengths were
462 extracted from MicrobeJ (rod and cocci) [55] or by manual tracing in Fiji (filaments).
463 Evaluations of statistical significance were performed using students T-tests in
464 GraphPad Prism software (v.9.2). Levels of significance are indicated as follows:
465 ns, not significant; *, $P < 0.05$; **, $P < 0.01$, ***, $P < 0.001$, ****, $P < 0.0001$

466

467 **Data availability**

468 - All data reported in this paper is available within the manuscript or its
469 supplementary material.
470 - This paper does not report original code.

471

472 **Acknowledgments**

473 The authors want to thank Prof. Danielle Garsin (University of Texas) for the *E. faecalis*
474 OG1RF strain and Prof. Scott Hultgren (University Washington in St. Louis) for the
475 *K. pneumoniae* TOP52 strain. B.S. acknowledge support from the Australian
476 Research Council through an ARC Future Fellowship (FT230100062). This study
477 received funding from internal UTS and Australian Institute for Microbiology and
478 Infection (AIMI) funding schemes to S.R. and B.S. The authors acknowledge the use

of the Leica Stellaris confocal microscope in the Microbial Imaging Facility at AIMI in the Faculty of Science, University of Technology Sydney.

Conflicts of interest

The authors declare no conflicts of interest.

Author contributions

B.S. conceptualised the study together with I.D.. C.A-K conduced the experiments together with B.S.. C.A-K and A.P constructed plasmids. I.D., C.A-K and B.S. analysed the data. S.A.R. and B.S. raised funding from UTS and AIMI for this project. C.A-K., A.P., I.D., and B.S contributed to the manuscript (writing and editing), all authors approved the final version.

492 **References**
493

494 1 Antimicrobial Resistance, C. Global burden of bacterial antimicrobial resistance
495 in 2019: a systematic analysis. *Lancet* **399**, 629-655, doi:10.1016/S0140-
496 6736(21)02724-0 (2022).
497 2 Flores-Mireles, A. L., Walker, J. N., Caparon, M. & Hultgren, S. J. Urinary tract
498 infections: epidemiology, mechanisms of infection and treatment options. *Nat*
499 *Rev Microbiol* **13**, 269-284, doi:10.1038/nrmicro3432 (2015).
500 3 Klein, R. D. & Hultgren, S. J. Urinary tract infections: microbial pathogenesis,
501 host-pathogen interactions and new treatment strategies. *Nat Rev Microbiol* **18**,
502 211-226, doi:10.1038/s41579-020-0324-0 (2020).
503 4 Shah, C., Baral, R., Bartaula, B. & Shrestha, L. B. Virulence factors of
504 uropathogenic Escherichia coli (UPEC) and correlation with antimicrobial
505 resistance. *BMC Microbiol* **19**, 204, doi:10.1186/s12866-019-1587-3 (2019).
506 5 Foxman, B. Urinary tract infection syndromes: occurrence, recurrence,
507 bacteriology, risk factors, and disease burden. *Infect Dis Clin North Am* **28**, 1-
508 13, doi:10.1016/j.idc.2013.09.003 (2014).
509 6 Xia, L. *et al.* Prevalence of ST1193 clone and IncI1/ST16 plasmid in E-coli
510 isolates carrying bla(CTX-M-55) gene from urinary tract infections patients in
511 China. *Scientific reports* **7**, 44866, doi:10.1038/srep44866 (2017).
512 7 Kucheria, R., Dasgupta, P., Sacks, S. H., Khan, M. S. & Sheerin, N. S. Urinary
513 tract infections: new insights into a common problem. *Postgraduate Medical*
514 *Journal* **81**, 83-86, doi:10.1136/pgmj.2004.023036 (2005).
515 8 Gaston, J. R., Johnson, A. O., Bair, K. L., White, A. N. & Armbruster, C. E.
516 Polymicrobial interactions in the urinary tract: is the enemy of my enemy my
517 friend? *Infect Immun*, doi:10.1128/IAI.00652-20 (2021).

518 9 Stickler, D. J. Bacterial biofilms in patients with indwelling urinary catheters. *Nat*
519 *Clin Pract Urol* **5**, 598-608, doi:10.1038/ncpuro1231 (2008).
520 10 Croxall, G. *et al.* Increased human pathogenic potential of Escherichia coli from
521 polymicrobial urinary tract infections in comparison to isolates from
522 monomicrobial culture samples. *J Med Microbiol* **60**, 102-109,
523 doi:10.1099/jmm.0.020602-0 (2011).
524 11 Kline, K. A. & Lewis, A. L. Gram-Positive Uropathogens, Polymicrobial Urinary
525 Tract Infection, and the Emerging Microbiota of the Urinary Tract. *Microbiol*
526 *Spectr* **4**, doi:10.1128/microbiolspec.UTI-0012-2012 (2016).
527 12 Rosen, D. A., Hooton, T. M., Stamm, W. E., Humphrey, P. A. & Hultgren, S. J.
528 Detection of intracellular bacterial communities in human urinary tract infection.
529 *PLoS Med* **4**, e329, doi:10.1371/journal.pmed.0040329 (2007).
530 13 Fourcade, C., Canini, L., Lavigne, J. P. & Sotto, A. A comparison of
531 monomicrobial versus polymicrobial Enterococcus faecalis bacteriuria in a
532 French University Hospital. *Eur J Clin Microbiol Infect Dis* **34**, 1667-1673,
533 doi:10.1007/s10096-015-2403-0 (2015).
534 14 de Vos, M. G. J., Zagorski, M., McNally, A. & Bollenbach, T. Interaction
535 networks, ecological stability, and collective antibiotic tolerance in polymicrobial
536 infections. *Proceedings of the National Academy of Sciences of the United*
537 *States of America* **114**, 10666-10671, doi:10.1073/pnas.1713372114 (2017).
538 15 Tien, B. Y. Q. *et al.* Enterococcus faecalis Promotes Innate Immune
539 Suppression and Polymicrobial Catheter-Associated Urinary Tract Infection.
540 *Infect Immun* **85**, doi:10.1128/IAI.00378-17 (2017).
541 16 Flores, C. *et al.* A human urothelial microtissue model reveals shared
542 colonization and survival strategies between uropathogens and asymptomatic

543 bacteria. *bioRxiv*, 2023.2006.2027.543376, doi:10.1101/2023.06.27.543376
544 (2023).
545 17 Jafari, N. V. & Rohn, J. L. An immunoresponsive three-dimensional urine-
546 tolerant human urothelial model to study urinary tract infection. *Frontiers in*
547 *cellular and infection microbiology* **13**, 1128132,
548 doi:10.3389/fcimb.2023.1128132 (2023).
549 18 Iosifidis, G. & Duggin, I. G. Distinct Morphological Fates of Uropathogenic
550 Escherichia coli Intracellular Bacterial Communities: Dependency on Urine
551 Composition and pH. *Infect Immun* **88**, doi:10.1128/IAI.00884-19 (2020).
552 19 Tandogdu, Z. *et al.* Antimicrobial resistance in urosepsis: outcomes from the
553 multinational, multicenter global prevalence of infections in urology (GPIU)
554 study 2003-2013. *World J Urol* **34**, 1193-1200, doi:10.1007/s00345-015-1722-
555 1 (2016).
556 20 Galvan, E. M., Mateyca, C. & Ielpi, L. Role of interspecies interactions in dual-
557 species biofilms developed in vitro by uropathogens isolated from polymicrobial
558 urinary catheter-associated bacteriuria. *Biofouling* **32**, 1067-1077,
559 doi:10.1080/08927014.2016.1231300 (2016).
560 21 Ganderton, L., Chawla, J., Winters, C., Wimpenny, J. & Stickler, D. Scanning
561 electron microscopy of bacterial biofilms on indwelling bladder catheters. *Eur J*
562 *Clin Microbiol Infect Dis* **11**, 789-796, doi:10.1007/BF01960877 (1992).
563 22 Desai, P. J., Pandit, D., Mathur, M. & Gogate, A. Prevalence, identification and
564 distribution of various species of enterococci isolated from clinical specimens
565 with special reference to urinary tract infection in catheterized patients. *Indian*
566 *J Med Microbiol* **19**, 132-137 (2001).

567 23 Macleod, S. M. & Stickler, D. J. Species interactions in mixed-community
568 crystalline biofilms on urinary catheters. *J Med Microbiol* **56**, 1549-1557,
569 doi:10.1099/jmm.0.47395-0 (2007).
570 24 Wang, X., Lünsdorf, H., Ehrén, I., Brauner, A. & Römling, U. Characteristics of
571 biofilms from urinary tract catheters and presence of biofilm-related
572 components in Escherichia coli. *Curr Microbiol* **60**, 446-453,
573 doi:10.1007/s00284-009-9563-z (2010).
574 25 Klumpp, D. J. *et al.* Uropathogenic Escherichia coli potentiates type 1 pilus-
575 induced apoptosis by suppressing NF-kappaB. *Infect Immun* **69**, 6689-6695,
576 doi:10.1128/IAI.69.11.6689-6695.2001 (2001).
577 26 Berry, R. E., Klumpp, D. J. & Schaeffer, A. J. Urothelial cultures support
578 intracellular bacterial community formation by uropathogenic Escherichia coli.
579 *Infect Immun* **77**, 2762-2772, doi:10.1128/IAI.00323-09 (2009).
580 27 Söderström, B., Pittorino, M. J., Daley, D. O. & Duggin, I. G. Assembly
581 dynamics of FtsZ and DamX during infection-related filamentation and division
582 in uropathogenic E. coli. *Nature communications* **13**, 3648,
583 doi:10.1038/s41467-022-31378-1 (2022).
584 28 Justice, S. S. *et al.* Differentiation and developmental pathways of
585 uropathogenic Escherichia coli in urinary tract pathogenesis. *Proceedings of*
586 *the National Academy of Sciences of the United States of America* **101**, 1333-
587 1338, doi:10.1073/pnas.0308125100 (2004).
588 29 Ballen, V., Ratia, C., Cepas, V. & Soto, S. M. Enterococcus faecalis inhibits
589 Klebsiella pneumoniae growth in polymicrobial biofilms in a glucose-enriched
590 medium. *Biofouling* **36**, 846-861, doi:10.1080/08927014.2020.1824272 (2020).

591 30 Justice, S. S., Hunstad, D. A., Seed, P. C. & Hultgren, S. J. Filamentation by
592 Escherichia coli subverts innate defenses during urinary tract infection.
593 *Proceedings of the National Academy of Sciences of the United States of*
594 *America* **103**, 19884-19889, doi:10.1073/pnas.0606329104 (2006).
595 31 Andersen, T. E. *et al.* Escherichia coli uropathogenesis in vitro: invasion,
596 cellular escape, and secondary infection analyzed in a human bladder cell
597 infection model. *Infect Immun* **80**, 1858-1867, doi:10.1128/IAI.06075-11 (2012).
598 32 Klein, K., Palarasah, Y., Kolmos, H. J., Moller-Jensen, J. & Andersen, T. E.
599 Quantification of filamentation by uropathogenic Escherichia coli during
600 experimental bladder cell infection by using semi-automated image analysis. *J*
601 *Microbiol Methods* **109**, 110-116, doi:10.1016/j.mimet.2014.12.017 (2015).
602 33 Rosen, D. A. *et al.* Utilization of an intracellular bacterial community pathway in
603 Klebsiella pneumoniae urinary tract infection and the effects of FimK on type 1
604 pilus expression. *Infect Immun* **76**, 3337-3345, doi:10.1128/IAI.00090-08
605 (2008).
606 34 Juarez, G. E. & Galván, E. M. Role of nutrient limitation in the competition
607 between uropathogenic strains of Klebsiella pneumoniae and Escherichia coli
608 in mixed biofilms. *Biofouling* **34**, 287-298,
609 doi:10.1080/08927014.2018.1434876 (2018).
610 35 Galván, E. M., Mateyca, C. & Ielpi, L. Role of interspecies interactions in dual-
611 species biofilms developed in vitro by uropathogens isolated from polymicrobial
612 urinary catheter-associated bacteriuria. *Biofouling* **32**, 1067-1077,
613 doi:10.1080/08927014.2016.1231300 (2016).
614 36 Gaston, J. R. *et al.* Enterococcus faecalis Polymicrobial Interactions Facilitate
615 Biofilm Formation, Antibiotic Recalcitrance, and Persistent Colonization of the

616 Catheterized Urinary Tract. *Pathogens* **9**, doi:10.3390/pathogens9100835
617 (2020).
618 37 Ch'ng, J. H. *et al.* Heme cross-feeding can augment Staphylococcus aureus
619 and Enterococcus faecalis dual species biofilms. *Isme j* **16**, 2015-2026,
620 doi:10.1038/s41396-022-01248-1 (2022).
621 38 Flores, C. *et al.* A human urothelial microtissue model reveals shared
622 colonization and survival strategies between uropathogens and commensals.
623 *Science Advances* **9**, eadi9834, doi:doi:10.1126/sciadv.adi9834 (2023).
624 39 Kao, P. H. *et al.* Enterococcus faecalis suppresses Staphylococcus aureus-
625 induced NETosis and promotes bacterial survival in polymicrobial infections.
626 *FEMS Microbes* **4**, xtad019, doi:10.1093/femsmc/xtad019 (2023).
627 40 Lavigne, J. P., Nicolas-Chanoine, M. H., Bourg, G., Moreau, J. & Sotto, A.
628 Virulent synergistic effect between Enterococcus faecalis and Escherichia coli
629 assayed by using the Caenorhabditis elegans model. *PLoS One* **3**, e3370,
630 doi:10.1371/journal.pone.0003370 (2008).
631 41 Tien, B. Y. Q. *et al.* Enterococcus faecalis Promotes Innate Immune
632 Suppression and Polymicrobial Catheter-Associated Urinary Tract Infection.
633 *Infection and Immunity* **85**, 10.1128/iai.00378-00317,
634 doi:doi:10.1128/iai.00378-17 (2017).
635 42 Keogh, D. *et al.* Enterococcal Metabolite Cues Facilitate Interspecies Niche
636 Modulation and Polymicrobial Infection. *Cell Host Microbe* **20**, 493-503,
637 doi:10.1016/j.chom.2016.09.004 (2016).
638 43 Ch'ng, J. H., Chong, K. K. L., Lam, L. N., Wong, J. J. & Kline, K. A. Biofilm-
639 associated infection by enterococci. *Nat Rev Microbiol* **17**, 82-94,
640 doi:10.1038/s41579-018-0107-z (2019).

641 44 Garsin, D. A. *et al.* in *Enterococci: From Commensals to Leading Causes of*
642 *Drug Resistant Infection* (eds M. S. Gilmore, D. B. Clewell, Y. Ike, & N.
643 Shankar) (2014).
644 45 Kau, A. L. *et al.* Enterococcus faecalis tropism for the kidneys in the urinary
645 tract of C57BL/6J mice. *Infect Immun* **73**, 2461-2468,
646 doi:10.1128/IAI.73.4.2461-2468.2005 (2005).
647 46 Shankar, N. *et al.* Role of Enterococcus faecalis surface protein Esp in the
648 pathogenesis of ascending urinary tract infection. *Infect Immun* **69**, 4366-4372,
649 doi:10.1128/IAI.69.7.4366-4372.2001 (2001).
650 47 Hughes, E. R. & Winter, S. E. Enterococcus faecalis: E. coli's Siderophore-
651 Inducing Sidekick. *Cell Host Microbe* **20**, 411-412,
652 doi:10.1016/j.chom.2016.09.018 (2016).
653 48 Montravers, P., Andremont, A., Massias, L. & Carbon, C. Investigation of the
654 potential role of Enterococcus faecalis in the pathophysiology of experimental
655 peritonitis. *J Infect Dis* **169**, 821-830, doi:10.1093/infdis/169.4.821 (1994).
656 49 Zhu Tan, C. A. *et al.* Enterococcus faecalis antagonizes Pseudomonas
657 aeruginosa growth in polymicrobial biofilms. *bioRxiv*, 2022.2001.2018.476859,
658 doi:10.1101/2022.01.18.476859 (2022).
659 50 Balleza, E., Kim, J. M. & Cluzel, P. Systematic characterization of maturation
660 time of fluorescent proteins in living cells. *Nature methods* **15**, 47-51,
661 doi:10.1038/nmeth.4509 (2018).
662 51 Shaner, N. C. *et al.* Improving the photostability of bright monomeric orange
663 and red fluorescent proteins. *Nature methods* **5**, 545-551,
664 doi:10.1038/nmeth.1209 (2008).

665 52 Watson, J. F. & Garcia-Nafria, J. In vivo DNA assembly using common
666 laboratory bacteria: A re-emerging tool to simplify molecular cloning. *J Biol*
667 *Chem* **294**, 15271-15281, doi:10.1074/jbc.REV119.009109 (2019).
668 53 Wright, K. *et al.* Mycobacterial infection-induced miR-206 inhibits protective
669 neutrophil recruitment via the CXCL12/CXCR4 signalling axis. *PLoS pathogens*
670 **17**, e1009186, doi:10.1371/journal.ppat.1009186 (2021).
671 54 Debroy, S. *et al.* Development of a genomic site for gene integration and
672 expression in Enterococcus faecalis. *J Microbiol Methods* **90**, 1-8,
673 doi:10.1016/j.mimet.2012.04.011 (2012).
674 55 Ducret, A., Quardokus, E. M. & Brun, Y. V. MicrobeJ, a tool for high throughput
675 bacterial cell detection and quantitative analysis. *Nat Microbiol* **1**, 16077,
676 doi:10.1038/nmicrobiol.2016.77 (2016).
677